

1 **Automating the quantification of coastal change using historical aerial photography: a case study**
2 **along the coastline of County Cork, Ireland**

3 Emma Chalençon^{ab*}, Fiona Cawkwell^a, Michael O'Shea^b, Jimmy Murphy^b

4 ^a Department of Geography, University College Cork, T12K8AF Cork, Ireland

5 ^b MaREI Centre, Environmental Research Institute (ERI), University College Cork, P43 C573 Cork, Ireland

6

7 * Corresponding author:

8 Emma Chalençon

9 emma.chalencon@ucc.ie (E. Chalencon).

10

11 **Keywords**

12 Aerial photography, Coastal monitoring, Shoreline change, Vegetation Line, Colour Vegetation Indices

13

14 **Abstract**

15 Coastlines worldwide are coming under increasing pressure due to climate change and human
16 activity. Data on shoreline change are essential for coastal managers and when no long-term
17 monitoring programs are implemented and shoreline change is typically on the order of less
18 than 1m/yr, as observed in Ireland, aerial photography is the most valuable source of
19 information. A well-established literature exists for automated vegetation extraction from

This peer-reviewed article has been accepted for publication but not yet copyedited or typeset, and so may be subject to change during the production process. The article is considered published and may be cited using its DOI.

10.1017/cft.2024.17

This is an Open Access article, distributed under the terms of the Creative Commons Attribution-NonCommercial-NoDerivatives licence (<http://creativecommons.org/licenses/by-nc-nd/4.0/>), which permits non-commercial re-use, distribution, and reproduction in any medium, provided the original work is unaltered and is properly cited. The written permission of Cambridge University Press must be obtained for commercial re-use or in order to create a derivative work.

20 digital images based on the near infrared reflectance, but there is less research available on
21 spectrally limited colour photography. This study develops a methodology for automating
22 vegetation line extraction from a series of historical aerial photography of the Cork coastline
23 in the South-West of Ireland. The approach relies on the Normalised Green–Blue Difference
24 Index (NGBDI), which is versatile enough to discriminate disparate coastal vegetation
25 environments, at different resolutions and in various lighting and seasonal conditions. An
26 iterative optimal threshold process and the use of LiDAR ancillary datasets resulted in an
27 automated vegetation line measurement with uncertainties estimated to be between 0.6 and
28 1.2m. Change rates derived from the vegetation lines extracted present uncertainties in the
29 range of $\pm 0.27\text{m/yr}$. This robust and repeatable method provides a valuable alternative to
30 time-consuming and subjective manual digitisation.

31

32 **Impact Statements**

33 Coastlines worldwide require effective management, and accurate, timely data on shoreline
34 movements are an indispensable prerequisite to inform the decisions made by coastal
35 managers. Field coastal monitoring requires considerable human resources, it is spatially
36 limited and time-consuming, but significantly it cannot be done retrospectively. In places
37 where no such programmes have been undertaken, Earth Observation satellite data can be
38 invaluable in capturing temporal changes. But where shoreline changes, or movement of the
39 vegetation line, is typically on the order of less than 1m per year, as observed in Ireland, aerial
40 photography is the most valuable source of regional to national scale information. While it is
41 common practice, manual digitisation of shorelines is subjective and time consuming.
42 Substantial literature is available on automated vegetation feature extraction using near-
43 infrared reflectance but, research on more spectrally limited RGB (red-green-blue) colour

44 photography, commonly acquired by aerial platforms, is limited to very high-resolution
45 Uncrewed Aerial Vehicles (UAV) photography. In this paper, we demonstrate the viability of
46 automated shoreline detection on aerial orthophotography making use of Colour Vegetation
47 Indices developed for UAV photography. Historical archives of aerial photography are
48 unevenly stocked with photography of varying quality and acquisition conditions, alongside
49 limited spectral content, making them challenging datasets to handle, but the methodology
50 developed has proved versatile enough to perform well at different resolutions, and in
51 different lighting and seasonal conditions, effectively discriminating diverse coastal vegetation
52 environments. This research provides a robust and repeatable method to extract shoreline
53 change information from data-limited archives.

54

55 **Introduction**

56 Following a worldwide pattern (UNEP, 2017), the highest concentrations of population and
57 activity in the Republic of Ireland are found in coastal areas with 1.9 million people residing
58 within 5km of the coast, representing 40 percent of its population (CSO, 2016). Human
59 activities coupled with a changing climate, associated with rising sea levels and an increase in
60 storminess, impact shoreline movements and can have major detrimental effects. Coastal
61 erosion and flooding can eventually lead to a loss of habitats and ecosystems, damage to a
62 range of infrastructure, and disruption to social and economic systems (IPCC, 2018). Coastlines
63 worldwide require ongoing effective management, and accurate, timely data on shoreline
64 movement are an indispensable prerequisite to inform the decisions made by coastal
65 managers.

66 In recent years in Ireland there has been a growing interest from stakeholders for accurate
67 data on coastal change to better address challenges faced by populations, infrastructures, and

68 ecosystems. This need was underscored in the Report of the Inter-Departmental Group on
69 National Coastal Change Management Strategy, published in October 2023, which identified
70 deficiencies, including the lack of monitoring along the majority of the national coastline
71 (Department of Housing, Local government and Heritage and the Office of Public Works,
72 2023). The most recent national coastal erosion assessment undertaken in Ireland was the
73 Irish Coastal Protection Strategy Study (RPS/ICPSS, 2011). The shoreline position was retrieved
74 from manual digitisation of aerial photography at different dates between 1973 and 2006
75 (RPS/ICPSS, 2011). Annual retreat rates were derived assuming a linear retreat process, and
76 the change in position of the shoreline was measured at a very coarse resolution of 1km. This
77 analysis is now outdated and must be extended in time to account for shoreline change which
78 has happened since 2006. Despite these limitations and the dataset's focus on identification
79 of retreating coastal segments, it has been the only quantitative reference used by local
80 authorities in Ireland since 2011 (Flood and Schechtman, 2014; McKibbin, 2016; Lawlor and
81 Cooper, 2024).

82 Consistent archives of coastal movements over multiple decades are rare. In the United
83 Kingdom, the East Riding Regional Coastal Monitoring Programme established in the late
84 1990s, with collections of beach cross-profiles at 75 different points along the coast every six
85 months, is an example of best practice (East Riding of Yorkshire Council, 2006). Moreover,
86 annual aerial photographs from the past two decades, available through the Channel Coast
87 Observatory (CCO), provide a valuable resource for large-scale shoreline change analysis,
88 complementing localized and resource-intensive field monitoring efforts. In places where no
89 monitoring programmes have been undertaken, maps are invaluable for shoreline change
90 analysis due to their historical significance. However, historical maps in Ireland are infrequent
91 and often lack precision, preventing their inclusion in the study and necessitating a reliance

92 on aerial photography. Ireland holds an archive of national photography captured periodically
93 since 1995. The spatial and spectral resolution of aerial photography acquired worldwide is
94 very varied, but typically, the older the aerial photography, the less detail is available, with the
95 first national campaign in Ireland only acquiring panchromatic photography for example.
96 Aerial photography acquired in three or more spectral bands are now more common, and in
97 Ireland, national photography was acquired in the Red, Green, and Blue (RGB) parts of the
98 electromagnetic spectrum up until 2013, after which the Near Infrared (NIR) was included.

99 In this study, shoreline will refer to the dynamic boundary where the land meets the sea, a
100 line subject to change from natural and human influences. The coastline encompasses the
101 entire length of land along the sea. Shoreline detection techniques are generally classified into
102 datum-based methods, which utilise LiDAR or other elevation capture technologies to create
103 digital terrain models (DTMs), and proxy-based methods (Pollard, Brooks, and Spencer 2019).
104 Datum-based methods are limited by infrequent image capture and inconsistent spatial
105 coverage (Pardo-Pascual et al. 2018), limitations which apply to Cork. Proxy-based methods
106 rely on the detection of visible indicators whether they are geomorphological, vegetation,
107 water or human features (Toure et al. 2019). The most frequently identified shoreline indicator
108 from optical images is the instantaneous waterline, as it is the most visually discernible feature
109 (McAllister *et al.* 2022). However, to use instantaneous waterlines as indicators of shoreline
110 change, they must be corrected using estimates of beach slope and tidal height timeseries,
111 which can be challenging to obtain in areas with observation gaps (Muir et al., 2024), such as
112 along the Cork coastline. On the contrary, the seaward edge of stable coastal vegetation, the
113 vegetation line, serves as a less variable shoreline proxy (Pollard et al., 2020), effectively
114 capturing changes without the bias introduced by tidal stages (Toure et al., 2019). While the
115 vegetation line may vary seasonally, it was selected as shoreline proxy given the study area

116 data limitations. Although this proxy is ineffective on artificial or hard cliff coasts, it is a
117 valuable indicator of shoreline change in soft, sandy environments, such as Cork, where storm
118 energy gradients drive coastal dynamics (Pollard et al., 2020; Devoy, 2008). Additionally,
119 remote sensing techniques for mapping vegetation have a well-established research history
120 (Ustin and Gamon, 2010). Vegetation is traditionally mapped with indices using NIR and red
121 reflectance. The normalised difference vegetation index (NDVI) is the most widely used metric
122 when it comes to quantifying the health and density of vegetation (Huang et al., 2021).
123 However, historical aerial photography do not commonly include NIR information.
124 The use of Colour Vegetation Indices (CVI) based only on RGB data grew with the
125 popularisation of UAV research. Most CVIs were thereby designed for centimetre scale
126 resolution photography. UAVs can play a significant role in monitoring and managing coastal
127 ecosystems (Joyce et al., 2023), however they cannot be acquired retrospectively to calculate
128 historical change rates. This research proposes a methodology to adapt the use of UAV-CVIs
129 to much coarser historical aerial photography for the purpose of historical vegetation line
130 identification.

131

132 **Study area and data**

133 *Study area*

134 The coastline of Ireland is very irregular with a bay-headland configuration resulting from a
135 high wave energy regime. Cork in the South-West of the Republic of Ireland has 1,094km of
136 coastline (Figure 1), and it is the county recording the highest proportion of its population
137 living within 100m of the coast (CSO, 2016). Cork has 422km of soft sandy coastline, and 91km
138 are at risk of erosion based on the results of the Ecopro (1996) and EuroSION (Salman, 2004)

139 projects. The eastern part of Cork's coastline is highlighted as more vulnerable due to its
140 geomorphological attributes and the higher recorded erosion rates in that area.

141 The methodology proposed to extract vegetation lines from historical aerial photography and
142 quantify shoreline change is applied to the entire Cork coastline. However, five sites along the
143 coast have been chosen to validate the results of this study (Figure 1). From East to West,
144 Pilmore and Garryvoe beaches were selected as two of the sites recording the highest retreat
145 rates in County Cork. Inchydoney and Owenahincha are two West Cork beaches with large
146 dune systems which make them very popular beaches. Finally, Garinish Bay hosts three small
147 sandy coves on the Beara Peninsula in the western part of County Cork.

148

149 *Aerial photography*

150 Tailte Éireann is the Irish agency in charge of national mapping. They completed their first full
151 coverage of the Republic of Ireland RGB aerial photography dataset in 2000. . From 2000
152 onwards, national coverage orthophotography datasets have been delivered periodically with
153 increasing spatial and spectral resolutions (Table 1).

154 Since field monitoring data exist only for a few sites for a single season and satellite imagery
155 are unsuitable due to the magnitude of change observed, aerial images are the most
156 valuable—and invariably the only—source of historical coastal positions in Ireland.
157 Nevertheless, working with aerial photography in Ireland can be highly challenging. Aligning
158 the availability of survey aircraft on the island with cloud-free weather conditions at times of
159 high sun angles in the summer season for the whole country is nearly impossible. Achieving
160 national coverage may entail flights spanning up to 5 years apart, occurring from March to
161 November. The exact time and date of acquisition for each photography is not always available

162 as these datasets have been produced by different contractors over the years with different
163 procedures and metadata requirements.

164 Aerial photography are orthorectified by the data provider, with each pixel having x and y co-
165 ordinates representing its position on the ground so that accurate measurements can be taken
166 from them, but the uncertainty varies between the datasets (Table 1, Column 5: “Positional
167 accuracy uncertainty (m)”).

168

169 *Complementary datasets*

170 Seaweed washed ashore and low-tide shallow waters might have similar spectral signatures
171 in the visible wavelengths to growing vegetation, therefore ancillary datasets have been used
172 to refine the study area and mask areas prone to misclassifications in low-lying areas. LiDAR
173 coverage of the Cork coastline is limited in frequency and spatial coverage, but several
174 datasets are available, each covering different sections of the coastline; the eastern Cork
175 coastline was surveyed as part of the Office of Public Works (OPW) Blom Coastal Survey in
176 2006-2007, Cork Harbour, as part of the OPW Flimap Survey in 2007 and the OPW Coastal
177 Aerial LiDAR survey covered the western part of the county’s coastline in 2021. To mask out
178 low-lying areas where misclassification issues can arise, all areas under 2m of elevation to the
179 Malin Head datum on the different LiDAR Digital Surface Models (DSMs) were merged to
180 create a low-lying areas mask. This threshold was determined through an iterative optimal
181 thresholding process, aimed at masking as much low-lying area as possible without
182 compromising the accommodation space for the vegetation line.

183 The choice of the vegetation line proxy for shoreline position is only relevant for soft coasts,
184 which are more vulnerable to change over time, and is not suitable for hard or artificial coasts
185 unless they are vegetated seaward. The previous coast classification work achieved by the

186 EuroSION (Salman et al, 2004) and the ICPSS (RPS, 2011) projects served as guidelines to
187 identify soft coastal segments. These were further refined using the National Land Cover Map
188 (NLCM), created by Tailte Éireann and the Environmental Protection Agency (EPA), and visual
189 inspection using the study photography database. This work resulted in a sandy shore
190 environments zone.

191

192 **Methods**

193 *Selecting a suitable CVI*

194 The use of vegetation indices is a common practice in remote-sensing studies, as they
195 minimise the influence of distorting factors (Ruiz, 1995) as well as combining and maximising
196 information from specific bands or parts of the electromagnetic spectrum. Several CVIs based
197 on colour RGB photography have been proposed to identify vegetation, primarily for data from
198 UAVs carrying RGB cameras. These CVIs include the normalised green-red difference index
199 (NGRDI) (Torres-Sanchez et al., 2013), the visible-band difference vegetation index (VDVI)
200 (Wang et al. 2015), the normalised green-blue difference index (NGBDI) (Wang et al. 2015)
201 and the Red-green-blue vegetation index (RGBVI) (Bendig et al. 2015).

202 The index chosen had to be versatile enough to perform well at different resolutions, and in
203 different lighting and seasonal conditions to discriminate very different vegetation
204 environments. The three coves of Garinish Bay backed by grass vegetation and the dunes from
205 the sandspit of Inchydoney (Figure 1) were chosen to test five different indices. The binary
206 classifications of vegetation or no vegetation resulting from the different indices were
207 assessed using the widely recognised overall accuracy metric, calculated as the total number
208 of correctly classified pixels divided by the total number of pixels in the reference data. Using
209 the 2000 photography (1m spatial resolution), the NGBDI (Equation (1)) outperformed the

210 NGRDI by 30%, the RGBVI by 5% and the VDVI by 9%, achieving 89% classification accuracy
211 when compared with manual photointerpretation. Using the 2018 photography (0.25m
212 spatial resolution), the NGBDI was once again the best performing index with an accuracy of
213 96%, similar to the 95% performance of the RGBVI. Since the 2018 photography also contained
214 NIR data, the performance of the NGBDI was compared to that of the commonly used
215 Normalised Difference Vegetation Index (NDVI), with a very similar accuracy of 94% achieved.
216 Using the 2021 photography (0.1m spatial resolution), all indices performed similarly with
217 accuracies of 97-98%, with the exception of the NGRDI, which had an accuracy of 79%. After
218 testing the different indices, the one which performed most consistently across the different
219 photography sets, gave the best statistical accuracy and generated the most coherent
220 vegetation line was the NGBDI (Eq. 1).

221

$$222 \quad \mathbf{NGBDI = (Green - Blue) / (Green + Blue)} \quad \mathbf{(1)}$$

223

224 The study's regional scope, the limited uniformity of sandy environments along the Cork
225 coastline, and large variations in data acquisition conditions precluded use of image
226 classification methods. The extensive training required, which would have to be undertaken
227 for each image set, would have negated the time-saving benefits of developing an automated
228 approach. To objectively differentiate between vegetation and non-vegetation pixels for the
229 varied environmental and acquisition conditions, an iterative optimal threshold process was
230 implemented, with different NGBDI thresholds tested, by visual examination of the spectral
231 signature of nearby pixels and defined according to the resolution of the dataset as well as
232 the seasonality of the acquisition date.

233 At 1m resolution, each pixel tends to represent a homogeneous area. With clear boundaries
234 and fewer mixed pixels, the distinction between features is more pronounced and higher
235 thresholds can be applied. A threshold value of 0.1 was chosen for both the 2000 and 2005
236 datasets.

237 At 0.25m resolution, more details are captured in the photography. Nevertheless, the
238 increased level of detail may not fully distinguish boundaries with intricate details and with
239 more mixed pixels, it becomes challenging to precisely delineate boundaries. As a result, a
240 more permissive threshold was needed to ensure that features of interest were captured
241 accurately. Therefore, thresholds of 0.08 and 0.06 were chosen for the 2011-2012 and the
242 2018 datasets respectively. The 2015 photography were treated separately from the 2018
243 photography given the season difference (April 2015 versus June 2018). The 2015
244 photography covers the Eastern part of Cork coastline, which is more homogeneous with
245 linear beaches backed by grass vegetation and no large dune systems. In April, grass is
246 reaching its growing peak, and its green reflectance is very distinctive. These conditions justify
247 the choice of a higher 0.15 threshold for the 2015 photography.

248 At 0.1m resolution, boundaries are more clearly defined, and features can be easily captured
249 on the 2021 photography. As a result, a higher threshold of 0.15 was applied to this dataset.

250

251 *From a binary photograph to a vegetation line*

252 Applying the selected threshold to the NGBDI output resulted in binary outputs of vegetation
253 pixels and background pixels, which had to be converted into a line feature for subsequent
254 input to the Digital Shoreline Analysis System (DSAS) (Himmelstoss et al., 2021). The binary
255 images were first polygonised then simplified using a double buffer process. First, a positive
256 buffer is applied, extending the vegetation polygon by a distance corresponding to the

257 photography's resolution. As a second step, a negative buffer is performed, contracting the
258 vegetation area by the same distance. This process helps smooth the vegetation edge,
259 simplifying its geometry.

260 Polygons under 8m^2 were usually identified as seaweed residuals or small patches of
261 vegetation not suitable to be integrated into the vegetation line. Based on this observation,
262 all polygons under 8m^2 and whose centroid lay within the National Land Cover Map's 'Exposed
263 Sediments' class were deleted. The remaining polygons were agglomerated using an
264 agglomeration distance of 10m, a minimum area of 80m^2 and a minimum hole area of
265 $10,000\text{m}^2$. They were finally converted into line features, and only lines within 50m of the
266 initial 2000 vegetation line were kept for the DSAS analysis. Vegetation lines were thus created
267 along the Cork coastline as proxies of shoreline position in 2000, 2005, 2011 or 2012, 2015 or
268 2018, and 2021. The full workflow can be seen in Figure 2.

269

270 *DSAS analysis*

271 The DSAS is a freely available software application that works within the Esri ArcGIS software
272 and calculates change statistics for a time series of shoreline vector spatial features
273 (Himmelstoss et al., 2021). The DSAS first requires a baseline to build transects along which
274 rates of change will be calculated. For consistency of measuring change using the data
275 available to this project, the 2000 vegetation line was selected. This baseline was categorised
276 as midshore, enabling transects to account for both retreat and accretion. The maximum
277 search distance was set to 30m to allow for large movements observed at sand spits, but
278 without transects intersecting each other in smaller coves. Transects were located at 10m
279 intervals and no smoothing distance was applied, as it tended to place transects
280 inappropriately parallel to the baseline. No manual editing or omission of transects crossing

281 the shorelines at oblique angles was performed, in order to make the process as automated
282 as possible and avoid manual intervention. This approach was feasible because, unlike the
283 overall sinuous Cork coastline, the soft shore segments are relatively straight. All statistics
284 available were calculated for each transect. The Shoreline Change Envelope (SCE) represents
285 the distance between the most seaward and the most landward shorelines that intersect a
286 specific transect. The end point rate (EPR) is calculated by dividing the SCE by the time elapsed
287 between the first and last dated shorelines that intersect a given transect. A linear regression
288 rate-of-change (LRR) statistic is calculated by fitting a least-squares regression line to all
289 shoreline points for a transect (Himmelstoss et al., 2021).

290

291 *Validation*

292 As no pre-existing dataset was available to validate the vegetation lines it was decided to
293 manually digitise vegetation lines for each available year at the five validation sites (Figure 1).
294 Points were generated every 25cm along the manually digitised vegetation lines, and at each
295 point the distance between the manually and automatically derived lines was recorded to
296 calculate the Mean Absolute Error (MAE).

297

298 **Results**

299 *Validating the automated detection of vegetation lines*

300 Vegetation lines were generated at every soft-shore site along the Cork coastline for 2000,
301 2005, 2011 or 2012, 2015 or 2018, and 2021 (Figure 3). The OPW Coastal Aerial Survey
302 acquired in 2021 is only available for sites West from Cork Harbour, therefore, five vegetation
303 lines were produced for the three sites West of Cork Harbour (Figure 3) and only four lines for

304 the two sites East of Cork Harbour (Figure 1). The Mean Absolute Error (MAE) and its
305 respective standard deviation for each site is recorded in Table 2.

306 The July 2000 vegetation lines record MAEs below one pixel across all sites, except for
307 Inchydoney, where the MAE slightly surpasses 1m at 1.09m due to some embryo dunes with
308 vegetation patches being omitted (Figure 4 - A). Given the relatively coarse resolution of the
309 orthophotography, the results accurately capture the vegetation lines at each site.

310 The results for the July 2005 vegetation lines are similar, with MAEs below one pixel across all
311 sites. The best outcomes are observed at Garryvoe beach with a MAE of 0.57m coupled with
312 a minimal standard deviation of 0.64m (Figure 4 – B). Garryvoe beach is backed by glacial tills
313 covered by agricultural fields. In July, these grasslands display a very distinctive green
314 reflectance, making it relatively easy to distinguish them from the sandy beach.

315 At the 0.25m spatial resolution of the November 2011 and March 2012 photography, several
316 sites show their largest MAEs. When remote sensing data are captured at a higher resolution,
317 it means that smaller and more complex details of the landcover are captured. However, there
318 is a critical point where the resolution might not be sufficient to capture the full complexity of
319 the landcover features. Real-world features are indeed often characterised by fractal patterns
320 that exhibit details at various scales. A discrepancy between the resolution and the complexity
321 of the landcover features may lead to misinterpretations or incomplete delineation of
322 landcovers. Inchydoney and Garryvoe beaches have MAEs slightly over 1m, and Owenahincha
323 beach records a 1.66m MAE with a large standard deviation at 2.16m. For all these sites, the
324 photography have been acquired in March, which is quite early in the spring season, and the
325 vegetation is not yet at its greenest, adding complexity to its detection.

326 At Owenahincha Beach in 2012, the vegetation line alternates between the most seaward
327 vegetation and more landward vegetation similar to that observed at Inchydoney beach. The

328 algorithm misses the pioneer marram grass, which has low contrast with the sand. This occurs
329 at a resolution that introduces additional inaccuracies, complicating precise boundary
330 delineation. It is important to note that although using manual digitisation as a validation
331 source in remote sensing is a legitimate approach, especially when alternative validation
332 sources are unavailable, it is subjective and may introduce its own set of inaccuracies.

333 The results obtained for the national orthophotography mosaic 2013-2018 are quite
334 heterogeneous. Just like Garryvoe beach, Pilmore is a long linear beach backed by grasslands
335 and 2015 is the year where its MAE is the lowest at 0.38m, or under two pixels of this dataset
336 (Figure 4 - D). Nevertheless, the issue related to embryo dunes and pioneer vegetation patches
337 is still present at Inchydoney beach in 2018, giving a MAE close to 3m (Table 2).

338 The last set of photography for 2021 is only available for the three sites West from Cork
339 Harbour. The spatial resolution is enhanced to 0.1m and the overall results are the best across
340 the different years. MAEs are below 0.75m across all sites, and below 0.6m at the three coves
341 of Garinish Bay (Figure 4 - E). The improved resolution captures additional complexity and
342 intricate details, allowing better differentiation between features, and reaching the fractal
343 analysis critical point where the complexity can fully be captured.

344

345 *Validating the resulting change rates.*

346 Although the validation of the extracted vegetation lines' position for each year is critical, it is
347 crucial to establish the degree to which positional errors, specific to each year, impact the
348 resultant change rates. For each of the five validation sites, a DSAS analysis was performed
349 using the manually digitised vegetation lines and compared with the DSAS analysis based on
350 the lines extracted using the automated method (Figure 5).

351 The average MAEs for End Point Rates across all sites is 0.24m/yr (Table 2). Given this result,
352 EPRs within the range $\pm 0.25\text{m/yr}$ may indicate a tendency towards stability rather than
353 change. When shoreline change lies within the error bounds, it is not possible to indicate
354 directional shoreline change (Pollard et al., 2020).

355 The dune system at Owenahincha beach shows MAEs around 0.25m (Table 2, Figure 5 – C).
356 The difference between the average rates calculated using both methods at Owenahincha is
357 under 0.05m/yr. Although it was one of the sites that showed the largest errors when
358 considering the positional accuracy of the individual automated vegetation lines, the embryo
359 dunes omitted one year are either fully integrated into the dune system or washed away on
360 the next photography, making little difference to the overall rates of vegetation line change.

361 Pilmore and Garinish Bay record the lowest MAEs (Table 2, Figure 5 – D & E), and average rates
362 at these sites show good agreement between the automated and manual approaches, with
363 differences of less than -0.05m/yr for Pilmore and 0.09m/yr for the three coves of Garinish
364 bay (Table 2). At Garryvoe beach, MAEs reach 0.37m (Table 2) and even though retreat is
365 indicated by both approaches, the difference in the average rates is 0.27m/yr (Table 2, Figure
366 5 – B). Unlike other sites, Garryvoe beach is backed by agricultural land. In some seasons some
367 of these fields were not vegetated and no vegetation line could be extracted for the most
368 western field on the 2011 and 2015 photography covering Garryvoe beach, which explains
369 why some lines erroneously veer north at the west end of Figure 5 – B. As the final
370 photography for this analysis is from 2015, a large error for this date can have greater
371 consequences for the final EPR of this specific part of the vegetation line. MAEs for the rest of
372 the vegetation line at Garryvoe beach show good agreements with the change rates derived
373 from manual digitisation (Figure 5 – B).

374

375

376

377 **Discussion**378 *A robust alternative to manual digitisation*

379 Historical aerial photographs are often the only available evidence of past coastal positions,
380 but their disparate quality, conditions of acquisitions, positional accuracy, and limited spectral
381 content make them challenging datasets to work with. This explains why many studies have
382 relied on manual digitisation. The last three national or regional studies on coastal change in
383 the Irish context made this choice; the OPW (RPS/ICPSS, 2011), the Geological Survey Ireland
384 (GSI) (GSI, 2023) and the Northern Ireland Historical Shorelines Analysis (NIHSA) project
385 (Grottoli et al., 2023). In a publication from 2021, Fabbri et al. report maximum digitising
386 errors arising from subjectivity of 0.3m for the Dune Foot Line and 0.85m for the Stable
387 Vegetation Line on UAV photography with a spatial resolution of 2-4 centimetres. The GSI's
388 National Assessment of Shoreline Change Report published in 2023, reports uncertainties in
389 vegetation line measurements of 1m, for the 2000 and 2005 datasets and 0.5m, for the 2005-
390 2012 and 2013-2018 datasets. Although the reported uncertainty for the two latter datasets
391 (0.5m) is slightly better than the 0.99m MAE given for the method presented here, the
392 uncertainty for the first two is comparable. Notably, the results from the GSI correspond to
393 the digitisation of County Dublin's coast where beaches tend to be longer and straighter than
394 the indented and varied coastline of County Cork. It is important to emphasise the subjective
395 nature of manual digitisation, whether employed for a final product or validation purposes,
396 especially in environments involving fragmented vegetation lines in dune systems. The
397 accuracy of the position or even the existence of a true vegetation line may be subject to
398 diverse interpretations from experts of equal knowledge.

399 Prior to this work, Cork County Council relied exclusively on ICPSS outcomes to guide
400 discussions and management of coastal risks. Of the five validation sites, only two had
401 available outputs. For Garryvoe, the ICPSS divided the area into two segments: the western
402 two-thirds indicated an erosion rate of 0.33m/yr, while the eastern third showed no erosion
403 (0m/yr). In contrast, the automated method used in this study returned an average EPR of -
404 0.85m/yr for the western segment and -0.25m/yr for the eastern end. Pilmore Beach was
405 covered by a single ICPSS segment, indicating an erosion rate of 0m/yr, whereas the
406 automated method revealed an average EPR of -0.40m/yr.

407 Regarding sites not flagged by the ICPSS, no clear dynamic patterns were observed at Garinish
408 Bay coves, as the rates fall within the margin of error. Owenahincha serves as an example of
409 best practice. After experiencing severe erosion in the 1970s (Mullane and MacSweeney
410 1977), the introduction of gabions, dune reshaping, and replanting stabilized the area, and
411 this study reveals the steadily advancing vegetation line, confirming the resilience of the
412 managed dunes. While local concerns about dune erosion arose at Inchydoney, the analysis
413 shows stable EPRs, with the 2000 shoreline more landward than the 2021 line. The most
414 significant changes occur at the western end, where the tip of the sand spit near the estuary
415 is retreating. These findings challenge perceptions of critical erosion while highlighting the
416 limitations of the EPR method. The steady retreat of the vegetation line since 2012 reveals a
417 more complex, non-linear pattern of shoreline dynamics, that could easily be missed without
418 intermediate aerial photographs.

419 While these findings provide valuable data on shoreline change, they offer only a partial view.
420 The next phase of the study will model near-shore conditions and sediment transport, and
421 these results will be incorporated into a Coastal Vulnerability Index (CVI), assessing hazard
422 exposure and susceptibility along the Cork coastline and linking coastal dynamics more

423 directly to vulnerable receptors. Nevertheless, this first phase of the study provides a more
424 nuanced and location-specific understanding of shoreline change, offering a significant
425 improvement that enables Cork County Council to make informed decisions based on actual
426 change data. Elementary GIS skills and minimal processing time and power are sufficient to
427 adapt and carry out this robust and repeatable automated vegetation line detection method
428 and produce ready-to-use and reliable change rates at a regional scale using a DSAS. The
429 transferability of the methodology elsewhere has been proven by its ability to deal with very
430 different coastal environments along the Cork coastline without using site-specific thresholds.
431 The method could be readily applied at a national scale, particularly since all the datasets used
432 provide national coverage. This method is a good illustration of Vitousek et al.'s (2023)
433 principle, where "data-poor" archives, with spatiotemporally sparse data of disparate quality
434 are turned into highly sought-after "data-rich" coastal science products. Another advantage
435 of this method lies in the limited data sources needed for the analysis. The addition of ancillary
436 data such as LiDAR and land cover, did not significantly affect the results, but did reduce
437 processing time with less manual cleaning of the results required. While additional LiDAR and
438 land cover datasets for each photography time period, could potentially help in rectifying
439 minor misclassifications, the overall impact on the results is likely negligible.

440

441 *Limitations and uncertainties*

442 A simple time-efficient automated method comes with limitations and uncertainties which
443 need to be clarified and considered when using the results. Uncertainty calculations are
444 essential when interpreting shoreline change rates, regardless of the method used to derive
445 them. These calculations involve uncertainties related to the photography positional accuracy
446 ranging here from 0.5 to 1m (Table 1), and the automated measurement uncertainties, which

447 have been estimated to be between 0.6 and 1.2m (Table 2) with a mean 95% confidence
448 interval of 0.98-1m. The combination of the photography positional accuracy and the
449 measurement uncertainties can be calculated using the square root of the sum of the two
450 uncertainties squared (Hapke et al., 2011). This gives results ranging from $\pm 0.6\text{m}$ for the 2021
451 dataset to $\pm 1.3\text{m}$ for the 2000 and 2005 datasets. Finally, the resulting shoreline change rate
452 measurement uncertainty has been estimated using a 95% confidence interval to be \pm
453 0.27m/yr , which is once again comparable to the manual digitisation uncertainties presented
454 by the GSI (2023). It is still valuable to draw robust conclusions from shoreline change with
455 relatively higher error terms when calculated over longer periods where the main shoreline
456 processes can be considered distinct from the errors (Pollard et al., 2020). The error terms
457 presented in this study are still much lower than the ones presented in recent remote sensing
458 studies on shoreline change with 2.37 to 7.97m for shorelines detected with VEdge_Detector
459 (Rogers *et al.* 2021) and 9.3 to 27.9m for delineations from VedgeSat (Muir *et al.* 2024). The
460 difference is largely explained by the resolution of the source images. VEdge_detector and
461 VedgeSat are working with satellite images with coarser resolutions and therefore larger
462 errors but over longer and denser timeseries unveiling different coastal dynamic processes.
463 Limitations have been identified in relation to specific environments and conditions. Dune
464 system progression can take the form of small embryo dunes which tend to be missed out by
465 the automated method. Change rates in these environments tend to be smoothed by the
466 method as early progression or washing away of the small dunes generally occurs. Seasonality
467 is an important parameter to take into consideration while working with vegetation features
468 using visible wavelengths. It is always easier to capture vegetation at its growing peak while it
469 is at its greenest, although the timing of this may differ for different vegetation species, and
470 indeed even between years depending on the weather. The marram grass in dune systems

471 and agricultural grasslands in Ireland do not display the same phenology. Marram grass' green
472 appearance is altered in July and August when it flowers, while grasslands reach their seasonal
473 peak in these months. Late autumn and early spring photography give poorer results.

474 The choice of a vegetation line to serve as shoreline-proxy is not always ideal as some back
475 beach environments might not always be vegetated, cultivated areas can be ploughed for
476 example and these misclassifications have greater consequences if they occur on the first or
477 last photography in the timeseries. Extra care and verification is needed in these instances.

478 However, the vegetation line was chosen as the best proxy option for the available data and
479 its effectiveness in detecting storm-driven changes (Pollard *et al.*, 2020), which are a
480 significant driver of shoreline change along the Cork coastline (Devoy, 2008). Finally, spatial
481 resolution is a critical parameter in any remote sensing workflow. This methodology is a good
482 illustration of the importance of recognising the fractal dimension of features of interest. An
483 improved resolution might not always improve results, and for many sites the 0.25m
484 photography gives poorer results than the 1m photography, while the 0.1m photography gives
485 the best outcomes due to complex vegetation edges being captured more precisely. This
486 finding suggests that future data collection should carefully consider the optimal resolution
487 for capturing boundary details. While higher resolutions may seem advantageous, they can
488 introduce inaccuracies at certain levels. Therefore, a lower resolution might be acceptable for
489 accurate boundary delineation without sacrificing detail (e.g., 1-m photography, as used in
490 this research). Identifying the ideal frequency and timing of aerial imagery acquisition is
491 challenging, as aerial imagery is typically collected for multiple purposes. Capturing shoreline
492 change using a vegetation line proxy is a specific application that would benefit from annual
493 acquisition, timed when the vegetation of interest has the greatest contrast with its
494 background. Though the optimal timing may vary depending on the area and vegetation type,

495 this study demonstrates that valuable insights can still be gained from aerial imagery even
496 when acquisition conditions are not ideal.

497

498 **Conclusion**

499 This research has demonstrated the viability of automated detection of vegetation lines on
500 aerial orthophotography, making use of CVIs developed for very high-resolution UAV
501 photography. The NGBDI proved to be versatile enough to distinguish the vegetation line for
502 very different temperate coastal vegetation environments on photography with different
503 spatial resolutions, acquired in different light and seasonal conditions. In most instances,
504 vegetation lines extracted using the automated method are within 1m of the manually
505 digitised line, with a measurement uncertainty similar to that achieved by manual digitisation,
506 even though the uncertainty of the automated method is more variable across the dataset.
507 The uncertainty is determined to be $\pm 0.27\text{m/yr}$ when looking at the consequent shoreline
508 change rates, which are the much-needed end products. This automated method provides a
509 reliable solution for local authorities and coastal managers with limited data sources, time,
510 and remote sensing knowledge.

511

512

513

514

515

516

517

518

519 **Acknowledgements**

520 The authors would like to thank Eamonn Mullaly and Tomas Kavanagh from Cork County
521 Council for facilitating access to the Tailte Eireann datasets as well as David Fahey from the
522 Office of Public Works for facilitating early access to the latest OPW datasets.

523 **Author Contribution Statement**

524 E. C. initially devised the methodology, performed all the analysis, and led the writing of the
525 article. F. C. contributed to method development, writing, and editing of the article, M. O.S.
526 and J. M. contributed to the supervision of the research and editing of the article.

527 **Conflict of interests**

528 None.

529 **Financial support**

530 This research was funded by Cork County Council Social Sustainability Infrastructure
531 Programme (SSIP) and the Department of Environment Climate Change under the Cork
532 Coastline Vulnerability Assessment project (2022-2026).

533 **Data availability**

534 The data that support the findings of this study are available from the corresponding author,
535 E.C., upon reasonable request, except for original data from Tailte Ireland and the OPW.

536

537

538

539

540

541

542

543 **References:**

544 **Bendig J, Yu K, Aasen H, Bolten A, Bennertz S, Broscheit J, Gnyp ML and Bareth G (2015)**

545 Combining UAV-based plant height from crop surface models, visible, and near infrared
546 vegetation indices for biomass monitoring in barley. *International Journal of Applied*
547 *Earth Observation and Geoinformation* **39**, 79–87.

548 <https://doi.org/10.1016/j.jag.2015.02.012>.

549 **Bhandari AK, Kumar A and Singh GK (2012)** Feature Extraction using Normalized Difference

550 Vegetation Index (NDVI): A Case Study of Jabalpur City. *Procedia Technology* **6**, 612–
551 621. <https://doi.org/10.1016/j.protcy.2012.10.074>.

552 **Buchailot MaL, Gracia-Romero A, Vergara-Diaz O, Zaman-Allah MA, Tarekegne A, Cairns**

553 **JE, Prasanna BM, Araus JL and Kefauver SC (2019)** Evaluating Maize Genotype
554 Performance under Low Nitrogen Conditions Using RGB UAV Phenotyping Techniques.
555 *Sensors* **19**(8), 1815. <https://doi.org/10.3390/s19081815>.

556 **Church JA and White NJ (2011)** Sea-Level Rise from the Late 19th to the Early 21st Century.

557 *Surveys in Geophysics* **32**(4–5), 585–602. <https://doi.org/10.1007/s10712-011-9119-1>.

558 **CSO - Central Statistics Office (n.d.) - Population Distribution (2016).**

559 <https://www.cso.ie/en/releasesandpublications/ep/p-cp2tc/cp2pdm/pd/> (accessed 8
560 May 2024)

561 **Department of Housing, Local Government and Heritage & the Office of Public Works**

562 (2023) *Report of the Inter-Departmental Group on National Coastal Change*
563 *Management Strateg*. Government of Ireland.

564 **Devoy RJN (2008)** Coastal Vulnerability and the Implications of Sea-Level Rise for Ireland.

565 *Journal of Coastal Research* **242**, 325–341. <https://doi.org/10.2112/07A-0007.1>.

- 566 **East Riding of Yorkshire Council** (2006) *Coastal Information Pack - Chapter 3 Coastal*
567 *Monitoring*. East Riding.
- 568 **ECOPRO (ed)** (1996) *Environmentally friendly coastal protection: code of practice*. Dublin:
569 Stationery Office.
- 570 **Fabbri S, Grottoli E, Armaroli C and Ciavola P** (2021) Using High-Spatial Resolution UAV-
571 Derived Data to Evaluate Vegetation and Geomorphological Changes on a Dune Field
572 Involved in a Restoration Endeavour. *Remote Sensing* **13**(10), 1987.
573 <https://doi.org/10.3390/rs13101987>.
- 574 **Fathipour H, Arefi H, Shah-Hosseini R and Moghadam H** (2019) Corn forage yield prediction
575 using unmanned aerial vehicle photography at mid-season growth stage. *Journal of*
576 *Applied Remote Sensing* **13**(3), 034503. <https://doi.org/10.1117/1.JRS.13.034503>.
- 577 **Flood S and Schechtman J** (2014) The rise of resilience: Evolution of a new concept in
578 coastal planning in Ireland and the US. *Ocean & Coastal Management* **102**, 19–31.
579 <https://doi.org/10.1016/j.ocecoaman.2014.08.015>.
- 580 **Gamon JA and Surfus JS** (1999) Assessing leaf pigment content and activity with a
581 reflectometer. *New Phytologist* **143**(1), 105–117. [https://doi.org/10.1046/j.1469-](https://doi.org/10.1046/j.1469-8137.1999.00424.x)
582 [8137.1999.00424.x](https://doi.org/10.1046/j.1469-8137.1999.00424.x).
- 583 **Geological Survey Ireland** (2023) *National Assessment of Shoreline Change*.
- 584 **Grottoli E, Biaisque M, Jackson D and Cooper J** (2023) *Northern Ireland Historical*
585 *Shorelines Analysis (NIHSA) Project*. Ulster University, Cromore Road, Coleraine, BT52
586 1SA (United Kingdom).
- 587 **Hapke CJ, Himmelstoss EA, Kratzmann M and Thieler ER** (2011) *National Assessment of*
588 *Shoreline Change: Historical Shoreline Change along the New England and Mid-Atlantic*
589 *Coasts* (Open-File Report). College of Marine Science.

- 590 **Himmelstoss EA, Henderson RE, Kratzmann MG and Farris AS (2021)** *Digital Shoreline*
591 *Analysis System (DSAS) Version 5.1 User Guide*. Reston, Virginia: U.S. Geological Survey.
- 592 **Huang S, Tang L, Hupy JP, Wang Y and Shao G (2021)** A commentary review on the use of
593 normalized difference vegetation index (NDVI) in the era of popular remote sensing.
594 *Journal of Forestry Research* **32**, 1–6. [https://doi.org/10.1007/s11676-020-01155-](https://doi.org/10.1007/s11676-020-01155-1)
595 [1](https://doi.org/10.1007/s11676-020-01155-1). **IPCC (2018)** *Global Warming of 1.5°C: IPCC Special Report on Impacts of Global*
596 *Warming of 1.5°C above Pre-industrial Levels in Context of Strengthening Response to*
597 *Climate Change, Sustainable Development, and Efforts to Eradicate Poverty*, 1st edn.
598 Cambridge University Press. <https://doi.org/10.1017/9781009157940>.
- 599 **Joyce KE, Fickas KC and Kalamandeen M (2023)** The unique value proposition for using
600 drones to map coastal ecosystems. *Cambridge Prisms: Coastal Futures* **1**, e6.
601 <https://doi.org/10.1017/cft.2022.7>.
- 602 **Larrinaga A and Brotons L (2019)** Greenness Indices from a Low-Cost UAV Photography as
603 Tools for Monitoring Post-Fire Forest Recovery. *Drones* **3**(1), 6.
604 <https://doi.org/10.3390/drones3010006>.
- 605 **Lawlor PJ and Cooper A (2024)** Mainstreaming Climate Change Considerations for Coastal
606 Areas into Spatial Planning Policies at National and Regional Level; the Example of
607 Ireland. <https://doi.org/10.2139/ssrn.4729469>..
- 608 **McAllister E, Payo A, Novellino A, Dolphin T and Medina-Lopez E (2022)** Multispectral
609 satellite imagery and machine learning for the extraction of shoreline indicators.
610 *Coastal Engineering* **174**, 104102. <https://doi.org/10.1016/j.coastaleng.2022.104102>.
- 611 **McKibbin D (2016)** Legislative and policy response to the risk of coastal erosion and flooding
612 in the UK and Ireland. *Northern Ireland Assembly (NIAR 274-16)*.

- 613 **Muir FME, Hurst MD, Richardson-Foulger L, Rennie AF and Naylor LA** (2024) VedgeSat: An
614 automated, open-source toolkit for coastal change monitoring using satellite-derived
615 vegetation edges. *Earth Surface Processes and Landforms* **49**(8), 2405–2423.
616 <https://doi.org/10.1002/esp.5835>.
- 617 **Mullane D and MacSweeney T** (1977) Land lost to the sea. [video].
618 <https://www.rte.ie/archives/2022/0721/1311458-cork-beach-erosion/> (accessed 9
619 October 2024)
- 620 **Pardo-Pascual J, Sánchez-García E, Almonacid-Caballer J, Palomar-Vázquez J, Priego De Los**
621 **Santos E, Fernández-Sarría A and Balaguer-Beser Á** (2018) Assessing the Accuracy of
622 Automatically Extracted Shorelines on Microtidal Beaches from Landsat 7, Landsat 8
623 and Sentinel-2 Imagery. *Remote Sensing* **10**(2), 326.
624 <https://doi.org/10.3390/rs10020326>.
- 625 **Pollard JA, Brooks SM and Spencer T** (2019) Harmonising topographic & remotely sensed
626 datasets, a reference dataset for shoreline and beach change analysis. *Scientific Data*
627 **6**(1), 42. <https://doi.org/10.1038/s41597-019-0044-3>.
- 628 **Pollard JA, Spencer T, Brooks SM, Christie EK and Möller I** (2020) Understanding spatio-
629 temporal barrier dynamics through the use of multiple shoreline proxies.
630 *Geomorphology* **354**, 107058. <https://doi.org/10.1016/j.geomorph.2020.107058>.
- 631 **Rogers MSJ, Bithell M, Brooks SM and Spencer T** (2021) VEdge_Detector: automated
632 coastal vegetation edge detection using a convolutional neural network. *International*
633 *Journal of Remote Sensing* **42**(13), 4805–4835.
634 <https://doi.org/10.1080/01431161.2021.1897185>.
- 635 **RPS** (2011) *Irish Coastal Protection Strategy Study Phase 3 - South Coast* (Work Packages 2, 3
636 & 4A - Technical Report No. IBE0071). OPW.

- 637 **Ruiz CP** (1995) *Elementos de Teledetección*. RA-MA S.A. Editorial y Publicaciones.
- 638 **Salman A, Lombardo S and Doody P** (2004) *Living with coastal erosion in Europe: Sediment*
639 *and Space for Sustainability PART I - Major findings and Policy Recommendations of the*
640 *EUROSION project* (No. 1). Directorate General Environment European Commission.
- 641 **Thenkabail PS, Smith RB and De Pauw E** (2000) Hyperspectral Vegetation Indices and Their
642 Relationships with Agricultural Crop Characteristics. *Remote Sensing of Environment*
643 **71**(2), 158–182. [https://doi.org/10.1016/S0034-4257\(99\)00067-X](https://doi.org/10.1016/S0034-4257(99)00067-X).
- 644 **Torres-Sánchez J, López-Granados F, De Castro AI and Peña-Barragán JM** (2013)
645 Configuration and Specifications of an Unmanned Aerial Vehicle (UAV) for Early Site
646 Specific Weed Management. *PLoS ONE* **8**(3), e58210.
647 <https://doi.org/10.1371/journal.pone.0058210>.
- 648 **Toure S, Diop O, Kpalma K and Maiga AS** (2019) Shoreline Detection using Optical Remote
649 Sensing: A Review. *ISPRS International Journal of Geo-Information* **8**(2), 75.
650 <https://doi.org/10.3390/ijgi8020075>.
- 651 **UNEP** (2017, August 18) Coastal zone management. [http://www.unep.org/explore-](http://www.unep.org/explore-topics/oceans-seas/what-we-do/working-regional-seas/coastal-zone-management)
652 [topics/oceans-seas/what-we-do/working-regional-seas/coastal-zone-management](http://www.unep.org/explore-topics/oceans-seas/what-we-do/working-regional-seas/coastal-zone-management)
653 (accessed 5 December 2023)
- 654 **Ustin SL and Gamon JA** (2010) Remote sensing of plant functional types. *New Phytologist*
655 **186**(4), 795–816. <https://doi.org/10.1111/j.1469-8137.2010.03284.x>.
- 656 **Vitousek S, Buscombe D, Vos K, Barnard PL, Ritchie AC and Warrick JA** (2023) The future of
657 coastal monitoring through satellite remote sensing. *Cambridge Prisms: Coastal*
658 *Futures* 1, e10. <https://doi.org/10.1017/cft.2022.4>.
- 659 **Wan L, Li Y, Cen H, Zhu J, Yin W, Wu W, Zhu H, Sun D, Zhou W and He Y** (2018) Combining
660 UAV-Based Vegetation Indices and Photography Classification to Estimate Flower

661 Number in Oilseed Rape. *Remote Sensing* **10**(9), 1484.

662 <https://doi.org/10.3390/rs10091484>.

663 **Wang C and Myint SW** (2015) A Simplified Empirical Line Method of Radiometric Calibration

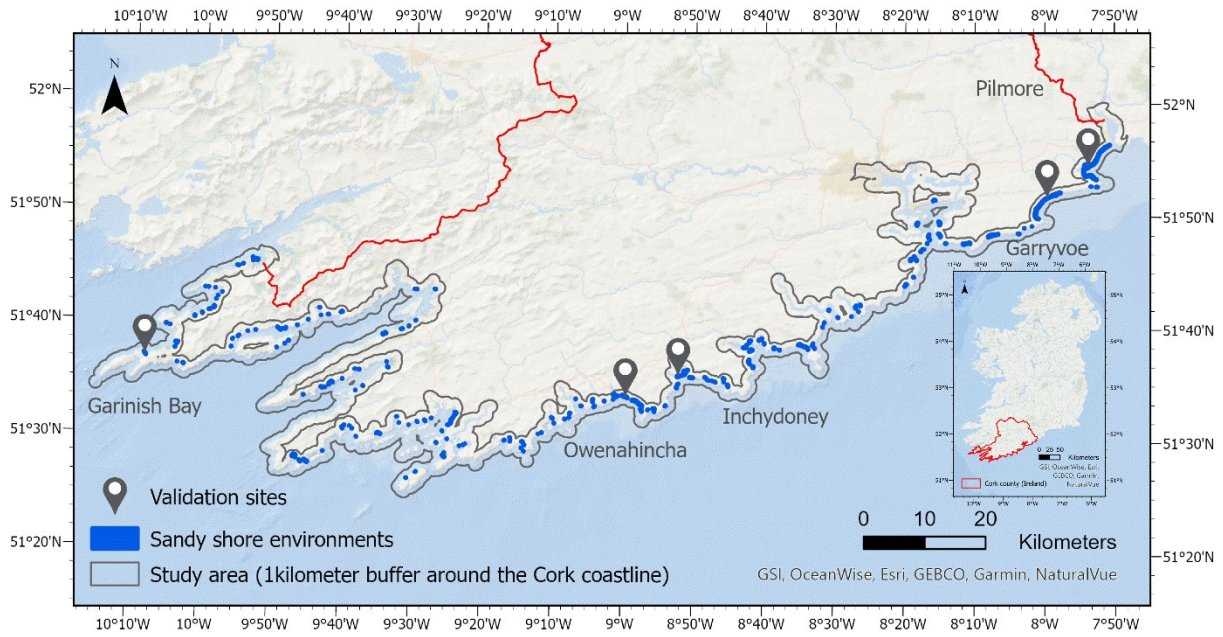
664 for Small Unmanned Aircraft Systems-Based Remote Sensing. *IEEE Journal of Selected*

665 *Topics in Applied Earth Observations and Remote Sensing* **8**(5), 1876–1885.

666 <https://doi.org/10.1109/JSTARS.2015.2422716>.

667

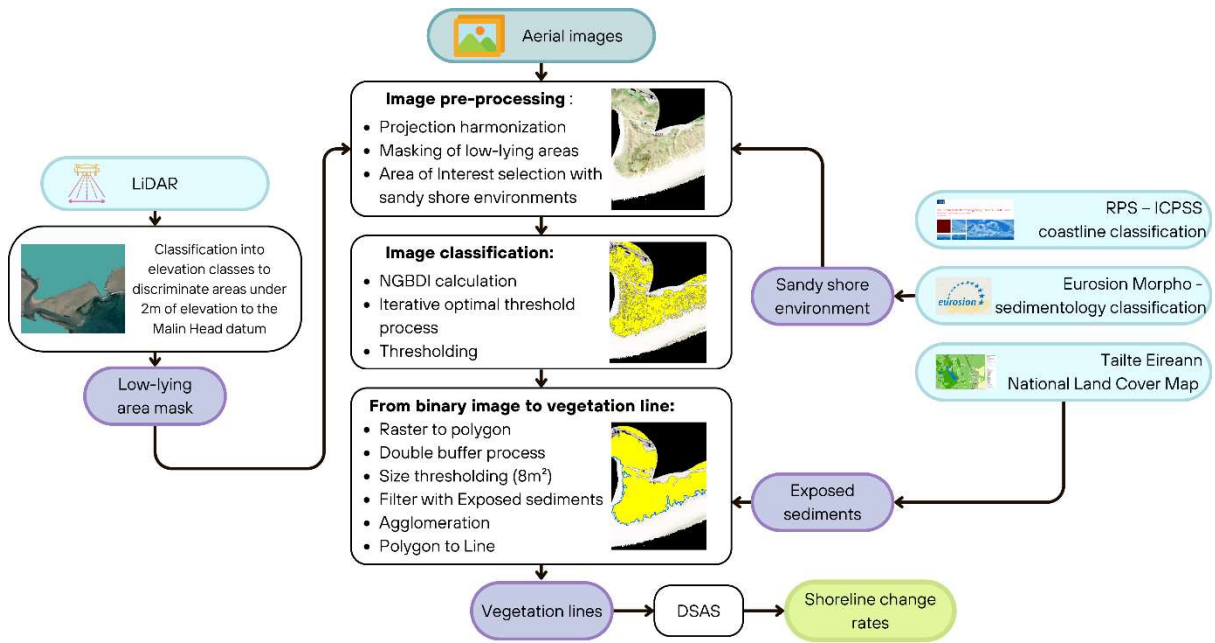
668 Figure 1



669

670

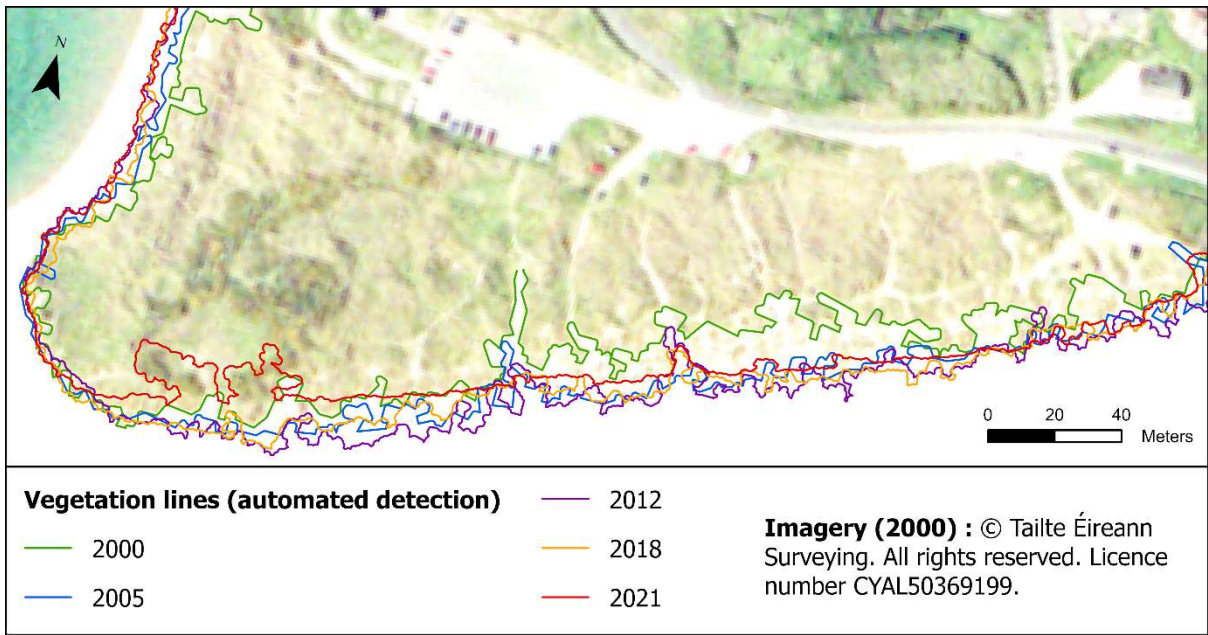
671 Figure 2



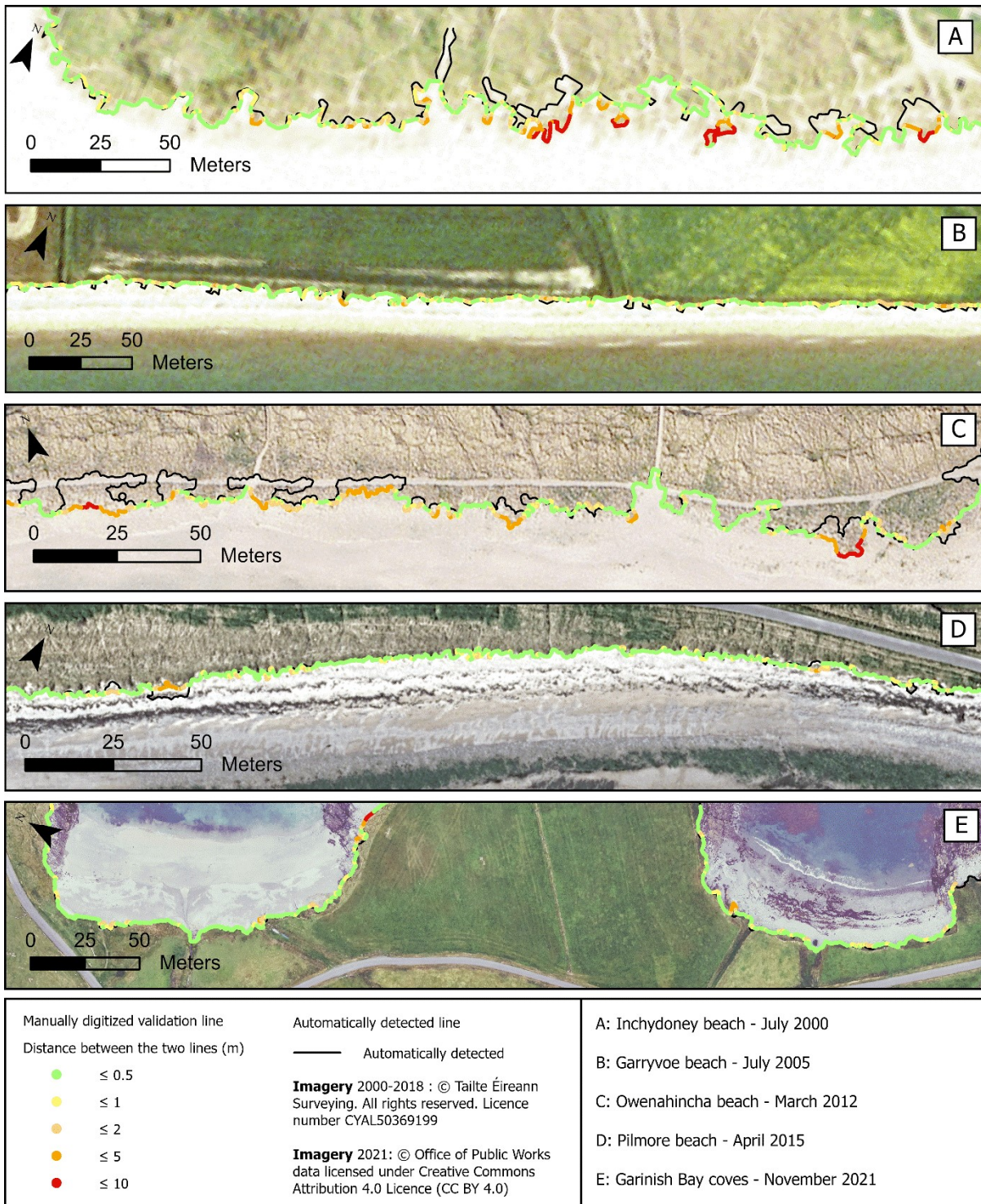
672

673

674 Figure 3



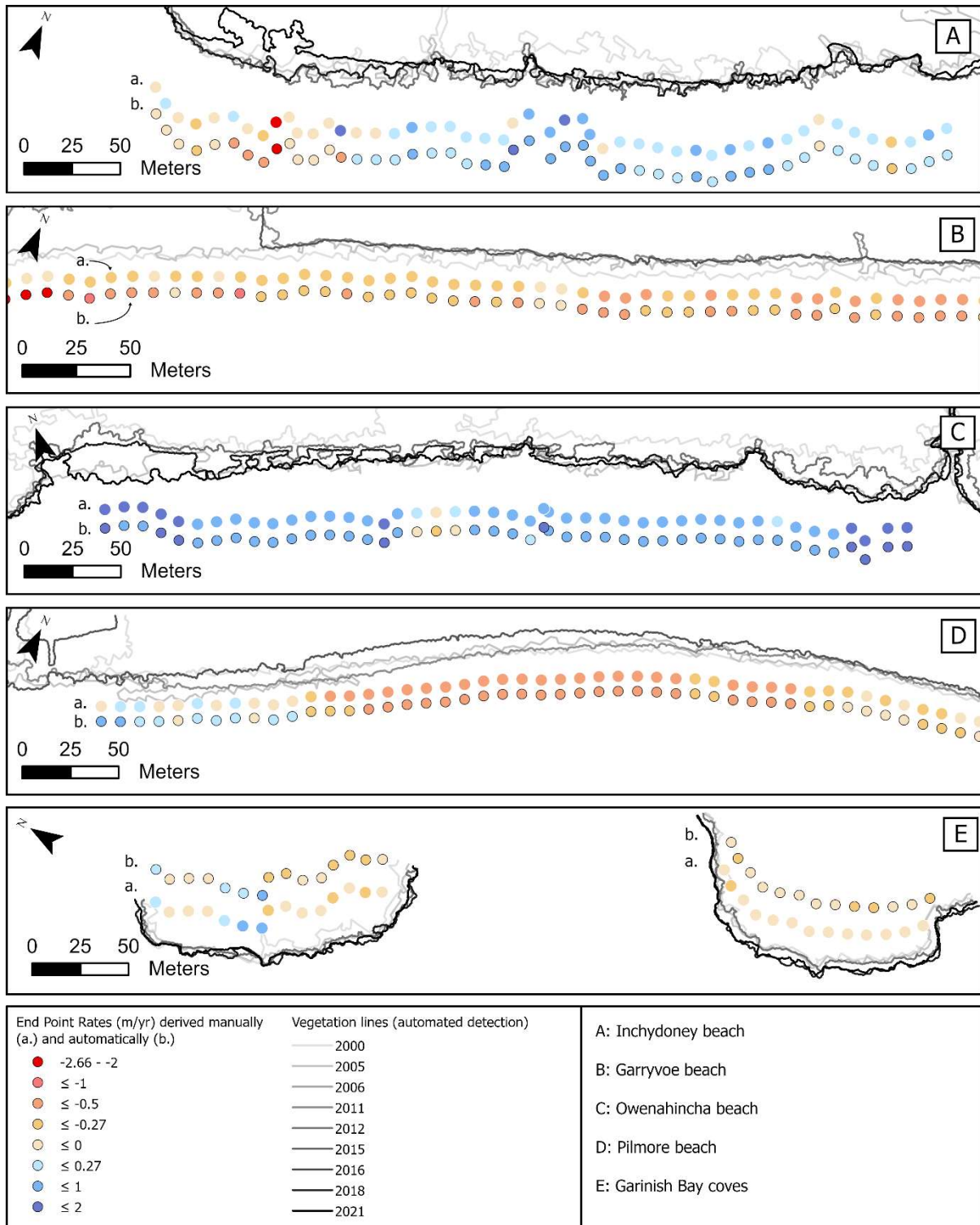
677 Figure 4



678

679

680 Figure 5



681